Thallium transport and the evaluation of olfactory nerve connectivity between the nasal cavity and olfactory bulb

Thallium transport and the evaluation of olfactory nerve connectivity between the nasal cavity and olfactory bulb

Yayoi Kinoshita[1], Hideaki Shiga[1]*, Kohshin Washiyama[2], Daisuke Ogawa[2], Ryohei Amano[2], Makoto Ito[1], Toshiaki Tsukatani[1], Mitsuru Furukawa[1] and Takaki Miwa[1]

Department of Otorhinolaryngology[1], Department of Forefront Medical Technology[2], Graduate School of Medical Science, Kanazawa University, 13-1 Takaramachi, Kanazawa, Ishikawa 920, JAPAN.

*Correspondence to be sent to: Hideaki Shiga, Department of Otorhinolaryngology, Graduate School of Medical Science, Kanazawa University, 13-1 Takaramachi, Kanazawa, Ishikawa 920, JAPAN.

Telephone: +81-076-265-2413. Fax: +81-076-234-4265

Email: shigah@med.kanazawa-u.ac.jp

Abstract

Little is known regarding how alkali metal ions are transported in the olfactory nerve following their intranasal administration. In this study, we show that an alkali metal ion, thallium is transported in the olfactory nerve fibers to the olfactory bulb in mice. The olfactory nerve fibers of mice were transected on both sides of the body under anesthesia. A double tracer solution (thallium-201, ^{201}Tl; manganese-54, ^{54}Mn) was administered into the nasal cavity the following day. Radioactivity in the olfactory bulb and nasal turbinate was analyzed with gamma spectrometry. Auto radiographic images were obtained from coronal slices of frozen heads of mice administered with ^{201}Tl or ^{54}Mn. The transection of the olfactory nerve fibers was confirmed with a neuronal tracer.

The transport of intranasal administered ^{201}Tl /^{54}Mn to the olfactory bulb was significantly reduced by the transection of olfactory nerve fibers. The olfactory nerve transection also significantly inhibited the accumulation of fluoro-ruby in the olfactory bulb. Findings indicate that thallium is transported by the olfactory nerve fibers to the olfactory bulb in mice. The assessment of thallium transport following head injury may provide a new diagnostic method for the evaluation of olfactory nerve injury.

Key words: Thallium, manganese, olfactory transport, alkali metal ions

Introduction

The clinical evaluation of olfactory function remains problematic. Many investigations have explored the use of newly developed instruments such as functional MRI (Koizuka et al. 1994; Sobel et al. 1998), magnetic encephalography (Tonoike al. 1998), positron emission tomography (Dade et al. 1998), olfactory event-related potential (Olofsson et al. 2006) or near-infrared spectroscopy (Kobayashi et al. 2007) to obtain objective olfactory function assessments. However, most of these methods have not advanced beyond the research laboratory and imaging the olfactory nerves presents significant technical challenges. Many physicians find it difficult to detect malingering among patients who seek compensation for olfactory problems related to head injury, because they don't have an objective test to evaluate olfactory function.

It is also difficult to predict prognosis of patients with olfactory dysfunction due to head injury. One reason is that the damage to olfactory nerve fibers can not be visualized with current magnetic resonance imaging (Fujii et al. 2002). Olfactory receptor neurons are bipolar cells with dendritic cilia processes extending toward the surface of the epithelium and small caliber axons less than a micron in diameter extending toward the brain. Olfactory neurons are located in the olfactory epithelium,

which lies just under the cribriform plate of the ethmoid bone that separates the nostril and cranial cavities. Olfactory nerve axons pass through the cribriform plate of the ethmoid bone to enter glomeruli within the olfactory bulb where they synapse on the dendrites of mitral and tufted cells (Kanayama et al. 2005). The axons of olfactory receptor neurons also provide a pathway by which ions can directly enter the brain (Mathison et al. 1998). It has been shown that the inhalation of manganese-54 (^{54}Mn) results in the extensive uptake of $^{54}Mn^{2+}$ by the olfactory bulb in rats (Brenneman et al. 2000). However, ^{54}Mn is not clear to be safely administered to patients because the half-life of ^{54}Mn is not short (312 days; da Silva et al. 2006). Manganese exposure is associated with Parkinson disease type neuronal degeneration (Bowler et al. 2007).

Thallium has been widely used with intravenous administration in isotope imaging for clinical diagnosis. We have shown that alkali metal ions as thallium-201 (^{201}Tl) administered intranasally is taken up into the olfactory epithelium, the olfactory bulb, and the cerebral cortex in mice (Kanayama et al. 2005). However, it is not clear whether ^{201}Tl is transported in the olfactory nerve fibers (the axons of olfactory receptor neurons) from the nasal cavity to the olfactory bulb. We have studied animal models of olfactory disturbance due to head injury (Miwa 1989; Tsukatani et al. 1995; Tsukatani et al. 2003).

In this study, we show the route of transport of ^{201}Tl to the olfactory bulb. We used intranasal administration of ^{201}Tl in mice after bilateral transection of the olfactory nerve fibers (BNTX) as an animal model. This model generates with olfactory disturbances similar to that due to head injury. Findings from this study suggest that nuclear imaging using intranasal administration of ^{201}Tl for patients with olfactory disturbance due to head injury warrant further development.

Materials and methods

Materials

Male ICR mice, eight weeks of age (Japan SLC, Shizuoka, Japan) were used in this study. They were housed in a 22^{o}C air-conditioned room with a 12:12 hour light-dark cycle and freely provided food (CHARLES RIVER LABORATORIES JAPAN, INC, Yokohama, Japan) and water. The Kanazawa University animal experiment committee approved all animal experimental procedures in advance (No.26142).

Methods

Transection of olfactory nerve fiber

The olfactory nerve fibers of mice were transected according to a method previously described (Costanzo 2000). We exposed both the right and left olfactory bulbs, cutting the frontal bones of mice under anesthesia (the inhalation of ether and intraperitoneal administration of pentobarbital sodium). The olfactory nerve fibers were transected bilaterally (BNTX) with a Teflon knife and scissors. The incision made in the skin was closed with a nylon suture.

^{201}Tl and ^{54}Mn experiments

^{201}TlCl saline solution (78 MBq/ml) was obtained from Nihon Medi-Physics (Kobe, Japan). $^{54}MnCl_2$ solution (37 MBq/ml, 1990 MBq/mg) was purchased from Perkin Elmer Life and Analytical Sciences (Boston, MA, USA). For *in vivo* experiments, these two tracer solutions were mixed as a double tracer solution (^{201}Tl, 39 MBq/ml; ^{54}Mn, 1.35MBq/ml; stable Mn, 0.15 mmol/ml).

The double tracer solution (20μl) was instilled into the right nostril. The mice were sacrificed under ether anesthesia 3 hours later. After samples of blood, the liver and kidney were obtained, head was dissected. Tissue samples were obtained from the head. The head was divided into four regions (the nasal turbinate, olfactory bulb, frontal brain, and rear brain). Separate samples from the right and left sides of the olfactory

bulb and brains were obtained for each region. Olfactory bulb, frontal brain and rear brain were assessed separately on the right and left sides.

The radioactivity of the samples was measured with gamma spectrometry using the Auto Well Gamma System (model ARC-380; Aloka, Tokyo, Japan) after weight measurement. The gamma spectrometry has a multi-channel analyzer discriminating the different energy levels of ^{201}Tl (72keV) and ^{54}Mn (835keV). The uptake percentage (%dose) of the isotope in each sample was calculated as a percentage of the radioactivity of each sample per the radioactivity of one percent of 20μl ^{201}TlCl/$^{54}MnCl_2$ solution. The ^{201}Tl/^{54}Mn uptake percentage per weight (%dose/g) was calculated as a percentage of the uptake percentage of each sample per wet weight.

The transport of ^{201}Tl/^{54}Mn by the olfactory nerve fibers was calculated as a percentage of the uptake percentage per weight (%dose/g) of the isotope in the right olfactory bulb divided by the isotope uptake percentage per weight (%dose/g) in the nasal turbinate. At least four mice each from the control and BNTX model were assessed.

Autoradiography

The mice were intranasally given the ^{201}TlCl or $^{54}MnCl_2$ solution for

autoradiography. Three hours later, the head was dissected. After removal of the skin and muscle, the head was embedded in Tissue-Tek OCT Compound (Sakura Finetechnical, Tokyo, Japan) and frozen in liquid nitrogen. The frozen heads were sectioned at 50μm. Coronal sections were obtained and dried. The sections were adhered to New CM-H film (Konica Medical, Tokyo, Japan) that was developed with a Konica X-ray Film Processor (Konica, Tokyo, Japan). Three control mice and three BNTX model mice were assessed for each isotope (Those mice were separately assessed from gamma spectrometry study).

Neuronal tracer experiment

Dextran tetramethylrhodamine (10μl of 50mg/ml solution; fluoro-ruby, 10,000MW, Molecular Probes, Invitrogen, Carlsbad, CA, USA) was injected into the right nasal epithelium. After 48h, the mice were sacrificed under ether anesthesia. The head of mice was dissected and the brain was embedded in Tissue-Tek OCT Compound and frozen. The accumulation of the tracer in the olfactory bulb was assessed in the sections (50μm) under a fluoroscopic microscope. Three control mice and three BNTX model mice were examined.

Statistical analysis

A statistical comparison of mean values was performed using the Student t-test (Prism 4, GraphPad, San Diego, CA, USA). All p values are two tailed. A p-value <0.05 was considered statistically significant.

Results

^{201}Tl / ^{54}Mn uptake after intranasal administration

The controls and BNTX models were intranasally administered with the double tracer solution (^{201}TlCl and ^{54} $MnCl_2$) because ^{54}Mn has been previously reported to transport from nasal cavity to olfactory bulb in rats (Brenneman et al. 2000). ^{201}Tl uptake percentage per weight (%dose/g) in the olfactory bulb and other organs of the mice 3 hours after the intranasal administration of the ^{201}TlCl solution is shown in Figure 1A. The uptake percentage per weight (%dose/g) of ^{201}Tl in the right olfactory bulb of the BNTX model was significantly reduced compared to the control ($P<0.005$). There were no significant differences in the uptake percentage per weight (%dose/g) of ^{201}Tl in blood, the liver and kidney, the frontal and rear brain, and the nasal turbinate between the BNTX model and the control.

Figure 1B shows ^{54}Mn uptake percentage per weight (%dose/g) in the olfactory

bulb and other organs of the mice 3 hours after a unilateral (right side) intranasal administration of the $^{54}MnCl_2$ solutions. The uptake percentage per weight (%dose/g) of ^{54}Mn in the right olfactory bulb of the BNTX model was significantly reduced relative to the control ($P<0.005$). There were no significant differences in the uptake percentage per weight in blood, the liver and kidney, the frontal and rear brain and nasal turbinate between the BNTX model and the control.

^{201}Tl and ^{54}Mn were transported to the olfactory bulb from the nasal cavity in the control mice. However, the uptake percentage per weight (%dose/g) of ^{201}Tl and ^{54}Mn in the olfactory bulb was significantly reduced in the BNTX model mice.

Transport of ^{201}Tl and ^{54}Mn between the nasal epithelium and olfactory bulb

To determine rate of transport of ^{201}Tl and ^{54}Mn between the nasal epithelium and olfactory bulb, we divided the uptake percentage per weight (%dose/g) in the right olfactory bulb (OBR) by the uptake percentage per weight (%dose/g) in nasal turbinate. The rate of transport of ^{201}Tl or ^{54}Mn between the nasal epithelium and olfactory bulb was significantly lower in the BNTX model than in the control (Figure 2; ^{201}Tl, $P<0.0001$; ^{54}Mn, $P<0.001$). ^{201}Tl and ^{54}Mn administered into the nasal epithelium were transported in the olfactory nerve fibers to the olfactory bulb.

^{201}Tl and ^{54}Mn transport images with autoradiography

To show the inhibition of ^{201}Tl and ^{54}Mn transport between the nasal epithelium and olfactory bulb with autoradiography, we assessed the isotope imaging with an intranasal administration of the ^{201}TlCl or $^{54}MnCl_2$ solution. It was found the transport of ^{201}Tl or ^{54}Mn was significantly inhibited with the transection of the olfactory nerve fibers in the BNTX model (Figure 3). Given the results of autoradiography, it appears that ^{201}Tl and ^{54}Mn administered into the nasal epithelium is transported by the olfactory nerve fibers.

Neuronal tracer accumulation in olfactory bulb of control and model

To verify whether the olfactory nerve fibers were completely transected in the BNTX model, we administered a neuronal tracer (fluoro-ruby) into the right nasal cavity. The accumulation of the tracer in the olfactory bulb was significantly prevented by the transection of the olfactory nerve fibers (Figure 4).

Discussion

We have shown that the transport of intranasally administered

thallium/manganese ions to the olfactory bulb was significantly decreased with the transection of olfactory nerve fibers in mice. It has been shown that ^{201}Tl is taken up in the region of the brain containing the olfactory tract, olfactory cortex, thalamus and hypothalamus after being introduced into the nasal cavity (Kanayama et al. 2005). In this study, ^{201}Tl was not yet taken up in the front and rear brain at three hours after intranasal administration of ^{201}Tl. From our results, ^{201}Tl transports in the olfactory nerve from the nasal cavity to the olfactory bulb of the mice because the transport of ^{54}Mn and neuronal tracer (fluoro-ruby) was also reduced in the BNTX model compared to the control.

We suppose that the uptake of ^{201}Tl reflects the behavior of potassium ion (K^+) channel and Na^+, K^+-ATPase, because thallium ion is an alkali metal ion. Therefore, $^{201}Tl^+$ may be transported from the nasal cavity to the olfactory bulb via axons and so must pass through the synaptic junction into the telencephalon and the diencephalon.

An ionic balance in neurons is crucial for normal functioning of the brain and is controlled by ionic transport across the blood-brain barrier, the choroids plexus and the membrane of glial cells and neurons (Strange 1992). The transport of metal ions as cadmium, nickel, and mercury in the olfactory system has been investigated. (Gottofrey and Tjalve 1991; Borg-Neczak and Tjalve 1996; Tjalv et al. 1996; Henrikssion et al.

1997; Tallkvist et al 1998;Henrikssion and Tjalve 1998).

Manganese ion (Mn^{2+}) has a similar ionic radius to calcium ion (Ca^{2+}) and its ability to affect neuronal transmission has been ascribed primarily to its mimicry of calcium (Aschner and Aschner 1991). Mn^{2+}has been shown to enter nerve terminals via calcium channels during nerve action potentials (Narita et al. 1990). Mn^{2+}also passes through calcium channels in myoepithelial cells (Anderson 1979). Mn^{2+} permeates presynaptic calcium channels and induces the release of dopamine from depolarized nerve endings (Drapeau and Naschsen 1984).

Considering our finding that the transport of ^{201}Tl or ^{54}Mn between the nasal epithelium and olfactory bulb was significantly inhibited with the transection of the olfactory nerve fibers in mice, thallium ion may be taken up into the olfactory receptor cells and transported in the olfactory nerve axon toward the olfactory bulb from the nasal epithelium similar to Mn^{2+}.

The mechanism of traumatic olfactory disturbance has been widely recognized as occurring due to (1) sinonasal contusions or nasal fractures; (2) tearing or shearing of the olfactory nerve fibers; and (3) intracranial confusion and hemorrhage in olfactory brain regions (Costanzo and Miwa 2006). Although the large pathological lesions in sinonasal tract or brain can be diagnosed with CT scan or MRI,

lesions of the olfactory fila, olfactory bulb or olfactory tract typically cannot be visualized. In addition, there are no methods to visualize the functional connections between the olfactory nerve and olfactory bulb. Intranasal administration of the ^{201}TlCl solution has the potential to be a clinical imaging test for the objective assessment of damage of olfactory nerve fibers. However, there are three problems that must be addressed, (1) safety issues when administered to the human nasal mucosa, (2) the correlation between the accumulations of ^{201}TlCl within olfactory brain centers and olfactory function, and (3) the visualization of the olfactory bulb and more central olfactory area within the brain. The ^{201}TlCl is administered safely in humans by intravenous injection. Our research is under investigation whether the intranasal administration of a ^{201}TlCl solution causes either histological or behavioral damage to the olfactory system. We are also presently investigating the correlation between ^{201}TlCl uptake in the olfactory bulb and olfactory function. We plan to adapt this procedure for use in humans after review and approval by the ethical committee for the Kanazawa University Hospital.

It has been shown that olfactory neurons regenerate by four weeks after the nerve transection in mammals (Costanzo et al. 1985; Miwa et al. 2002). In humans, the recovery rate in patients with traumatic olfactory dysfunction in less 30% (Fujii et al.,

2002). If we could adapt thallium imaging for patients by a simple intranasal administration, it may be possible to better diagnosis injuries to the olfactory nerves. In addition, if studies show that olfactory ability is correlated with transport of ^{201}Tl from the nasal cavity to the olfactory bulbs, this would also be of diagnostic value.

Acknowledgement

This research was supported in part by a research grant for young investigators in Kanazawa University (No.1817211 to H.S.; No.1816220 to K.W.) and a Grant-in-Aid for Scientic Research from the Ministry of Education, Science and Culture of Japan (C18591860 to T.M.).

References

Anderson M. 1979. Mn^{2+} ions pass through Ca^{2+} channels in myoepithelial cells. J Exp Biol 82: 227-38.

Aschner M, Aschner JL. 1991. Manganese neurotoxicity: cellular effects and blood-brain barrier transport. Neurosci Biobehav Rev 15: 333-40.

Borg-Neczak K, Tjalve H. 1996. Uptake of $^{203}Hg^{2+}$ in the olfactory system in pike. Toxicol Lett 84: 107-12.

Bowler RM, Roels HA, Nakagawa S, Drezgic M, Park R, Koller W, Bowler RP, Mergler D, Bouchard M, Smith D, Gwiazda R, Doty RL. 2007 Dose-effect relationships between manganese exposure and neurological, neuropsychological and pulmonary function in confined space bridge welders. Occup Environ Med 64: 167-77.

Brenneman KA, Wong BA, Buccellato MA, Costa ER, Gross EA, Dorman DC. 2000. Direct olfactory transport of inhaled manganese ((54)MnCl(2)) to the rat brain: toxicokinetic investigations in a unilateral nasal occlusion model. Toxicol Appl Pharmacol 169: 238-48.

Costanzo RM. 1985. Neural regeneration and functional reconnection following olfactory nerve transection in hamster. Brain Res 361: 258-66.

Costanzo RM. 2000. Rewiring the olfactory bulb: changes in odor maps following

recovery from nerve transection. Chem Senses 25: 199-205.

Costanzo RM, Miwa T. 2006. Posttraumatic olfactory loss. Adv Otorhinolaryngol 63: 99-107.

Dade LA, Jones-Gotman M, Zatorre RJ, Evans AC. 1998. Human brain function during odor encoding and recognition. A PET activation study. Ann N Y Acad Sci 855: 572-74.

da Silva MA, Poledna R, Iwahara A, da Silva CJ, Delgado JU, Lopes RT. 2006. Standardization and decay data determinations of 125I, 54Mn and 203Hg. Appl Radiat Isot 64: 1440-45.

Drapeau P, Nachshen DA. 1984. Manganese fluxes and manganese-dependent neurotransmitter release in presynaptic nerve endings isolated from rat brain. J Physiol 348: 493-510.

Fujii M, Fukazawa K, Takayasu S, Sakagami M. 2002. Olfactory dysfunction in patients with head trauma. Auris Nasus Larynx 29: 35-40.

Gottofrey J, Tjalve H. 1991. Axonal transport of cadmium in the olfactory nerve of the pike. Pharmacol Toxicol 69: 242-52.

Henriksson J, Tallkvist J, Tjalve H. 1997. Uptake of nickel into the brain via olfactory neurons in rats. Toxicol Lett 91: 153-62.

Henriksson J, Tjalve H. 1998. Uptake of inorganic mercury in the olfactory bulbs via olfactory pathways in rats. Environ Res 77: 130-40.

Kanayama Y, Enomoto S, Irie T, Amano R. 2005. Axonal transport of rubidium and thallium in the olfactory nerve of mice. Nucl Med Biol 32: 505-12.

Kobayashi E, Kusaka T, Karaki M, Kobayashi R, Itoh S, Mori N. 2007. Functional optical hemodynamic imaging of the olfactory cortex. Laryngoscope 117: 541-46.

Koizuka I, Yano H, Nagahara M, Mochizuki R, Seo R, Shimada K, Kubo T, Nogawa T. 1994. Functional imaging of the human olfactory cortex by magnetic resonance imaging. ORL J Otorhinolaryngol Relat Spec 56: 273-75.

Mathison S, Nagilla R, Kompella UB. 1998. Nasal route for direct delivery of solutes to the central nervous system: fact or fiction? J Drug Target 5: 415-41.

Miwa T. 1989. Study of behavioral and histological change in mice following olfactory nerve section. J Juzen Med Soc 98: 391-414.

Miwa T, Moriizumi T, Horikawa I, Uramoto N, Ishimaru T, Nishimura T, Furukawa M. 2002. Role of nerve growth factor in the olfactory system. Microsc Res Tech 58: 197-203.

Narita K, Kawasaki F, Kita H. 1990. Mn and Mg influxes through Ca channels of motor nerve terminals are prevented by verapamil in frogs. Brain Res 510: 289-95.

Olofsson JK, Broman DA, Gilbert PE, Dean P, Nordin S, Murphy C. 2006. Laterality of the olfactory event-related potential response. Chem Senses 31: 699-704.

Sobel N, Prabhakaran V, Desmond JE, Glover GH, Goode RL, Sullivan EV, Gabrieli JD 1998. Sniffing and smelling: separate subsystems in the human olfactory cortex. Nature 392: 282-86.

Strange K. 1992. Regulation of solute and water balance and cell volume in the central nervous system. J Am Soc Nephrol 3: 12-27.

Tallkvist J, Henriksson J, d'Argy R, Tjalve H. 1998. Transport and subcellular distribution of nickel in the olfactory system of pikes and rats. Toxicol Sci 43: 196-203.

Tjalve H, Henriksson J, Tallkvist J, Larsson BS, Lindquist NG. 1996. Uptake of manganese and cadmium from the nasal mucosa into the central nervous system via olfactory pathways in rats. Pharmacol Toxicol 79: 347-56.

Tonoike M, Yamaguchi M, Kaetsu I, Kida H, Seo R, Koizuka I. 1998. Ipsilateral dominance of human olfactory activated centers estimated from event-related magnetic fields measured by 122-channel whole-head neuromagnetometer using odorant stimuli synchronized with respirations. Ann N Y Acad Sci 855: 579-90.

Tsukatani T, Furukawa M, Moriya M, Tanaka S, Okoyama S, Moriizumi T. 1995. Bulbar morphology and expression of bulbar dopamine and parvalbumin in

experimentally-induced anosmic rats. Acta Otolaryngol 115: 539-42.

Tsukatani T, Fillmore HL, Hamilton HR, Holbrook EH, Costanzo RM. 2003. Matrix metalloproteinase expression in the olfactory epithelium. Neuroreport 14: 1135-40.

Figure legends

Figure 1

The uptake percentage (%dose) of the isotope in each sample was calculated as a percentage of the radioactivity of each sample per the radioactivity of one percent of 20μl $^{201}TlCl/^{54}MnCl_2$ solution.

(A) ^{201}Tl uptake percentage per weight (%dose/g) after a unilateral (right side) intranasal administration of the $^{201}TlCl$ solution in the control (N=4) and BNTX model (N=4). Data are the mean±S.D. (B) ^{54}Mn uptake percentage per weight (%dose/g) after a unilateral (right side) intranasal administration of the $^{54}MnCl_2$ solution in the control (N=4) and BNTX model (N=4). All data are the mean±S.D. A log scale was used on the Y-axis (A and B).

Figure 2

The rate of transport of ^{201}Tl or ^{54}Mn from the nasal cavity to the right olfactory bulb (OBR) after an intranasal administration in the control (N=4) and BNTX model (N=4). The rate of transport of ^{201}Tl or ^{54}Mn in the olfactory nerve was significantly higher in the control than in the BNTX model (^{201}Tl, ***P<0.0001; ^{54}Mn, **P<0.001). Data are reported as the mean±S.D.

Figure 3

Representative frozen sections and isotope images of coronal sections of the head at 3 hours after a unilateral (right side) intranasal administration of the ^{201}TlCl or ^{54} $MnCl_2$solution. Dotted arrows indicate the olfactory bulb and solid arrows, the nasal cavity.

Figure 4

Representative images of fluoro-ruby's accumulation in the olfactory bulb in Control and the absence of accumulation in the BNTX model after a nasal administration.

Figure 1

A

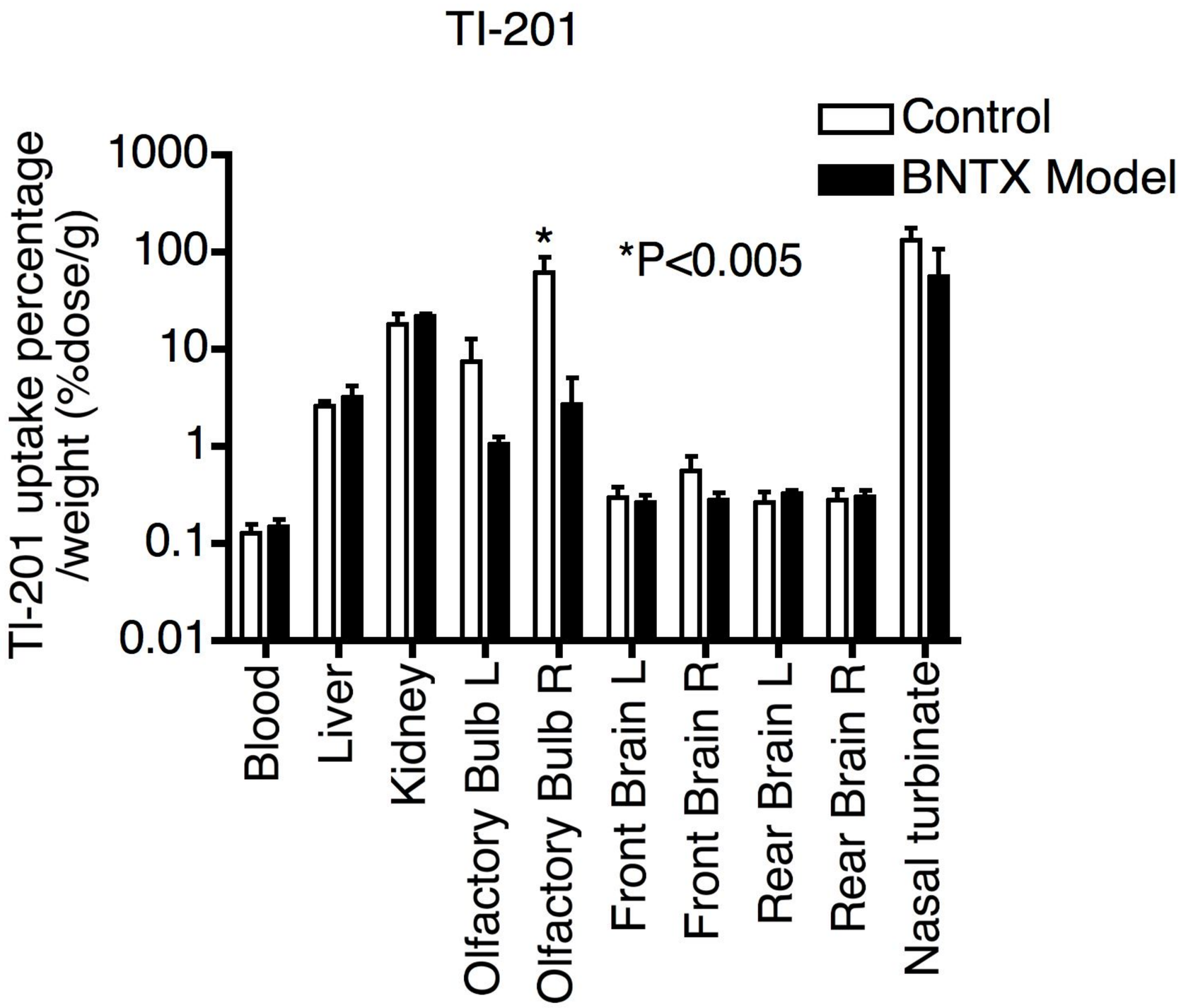
TI-201
Control
BNTX Model
*P<0.005
*
TI-201 uptake percentage /weight (%dose/g)
1000
100
10
1
0.1
0.01
Blood
Liver
Kidney
Olfactory Bulb L
Olfactory Bulb R
Front Brain L
Front Brain R
Rear Brain L
Rear Brain R
Nasal turbinate

B

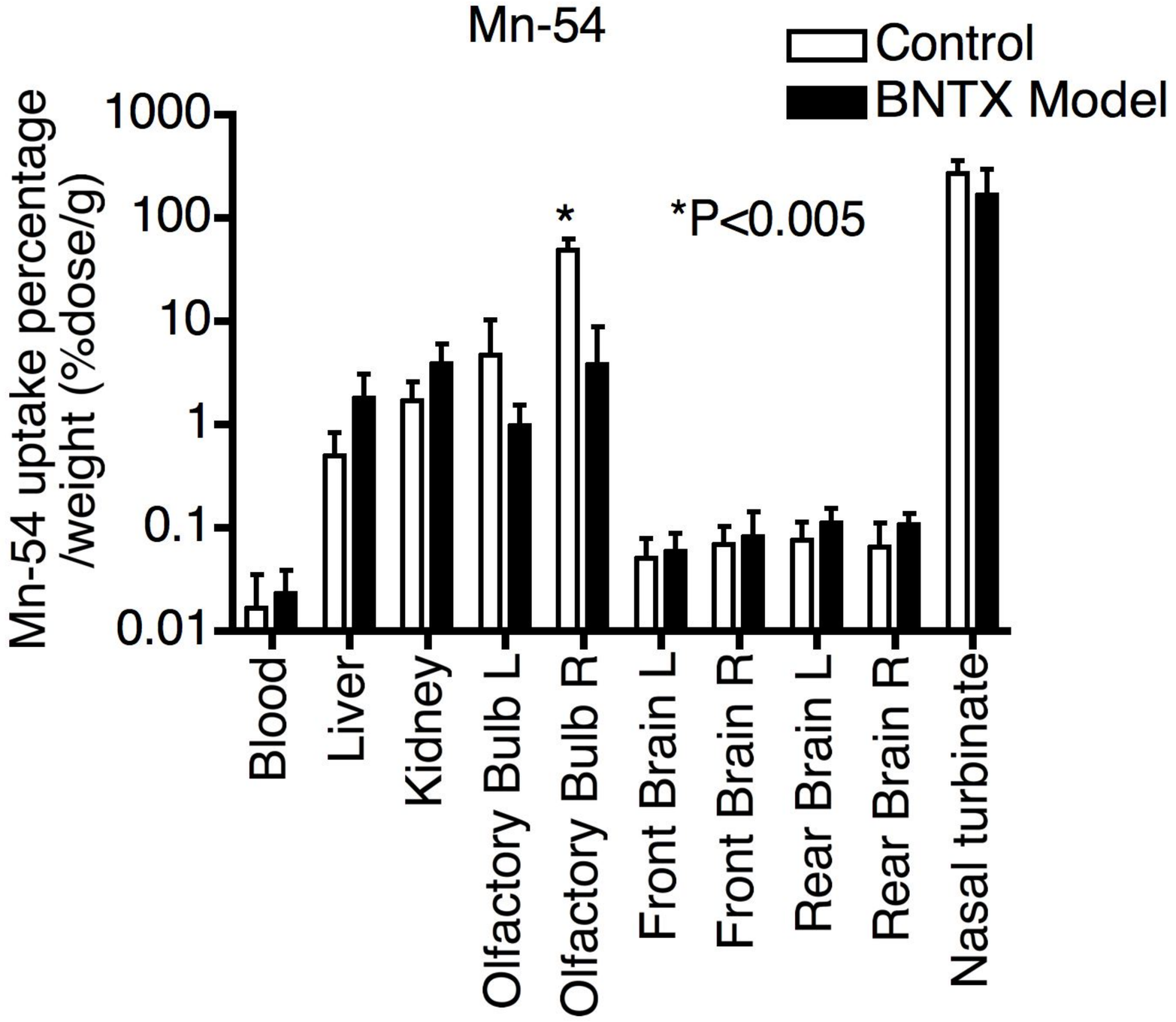
Mn-54
Control
BNTX Model
*P<0.005
*
Mn-54 uptake percentage /weight (%dose/g)
1000
100
10
1
0.1
0.01
Blood
Liver
Kidney
Olfactory Bulb L
Olfactory Bulb R
Front Brain L
Front Brain R
Rear Brain L
Rear Brain R
Nasal turbinate

Figure 2

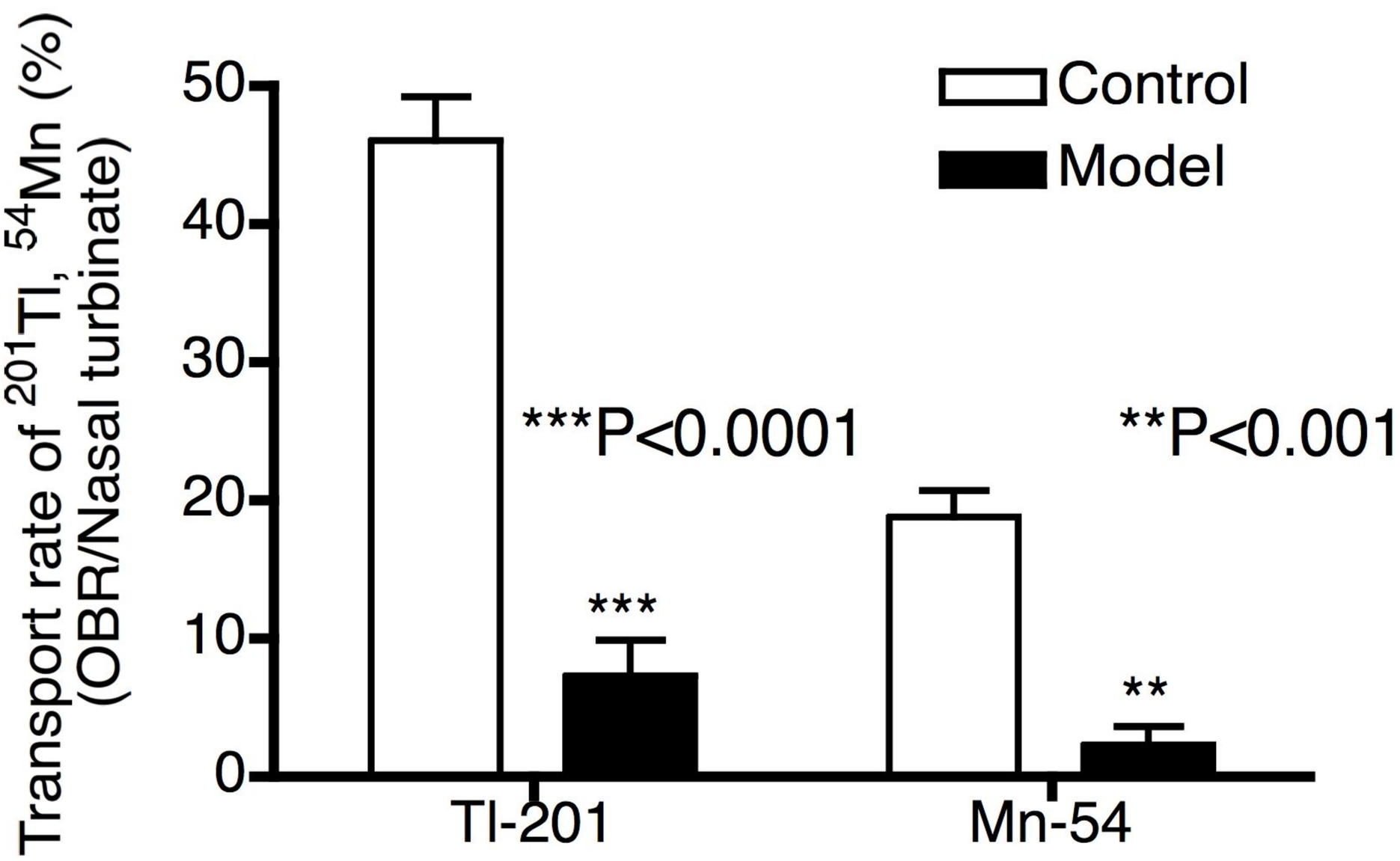
Transport rate of ^{201}Tl, ^{54}Mn (%)
(OBR/Nasal turbinate)
50
40
30
20
10
0
Control
Model
***P<0.0001
**P<0.001
***
**
Tl-201
Mn-54

Figure 3

Tl-201

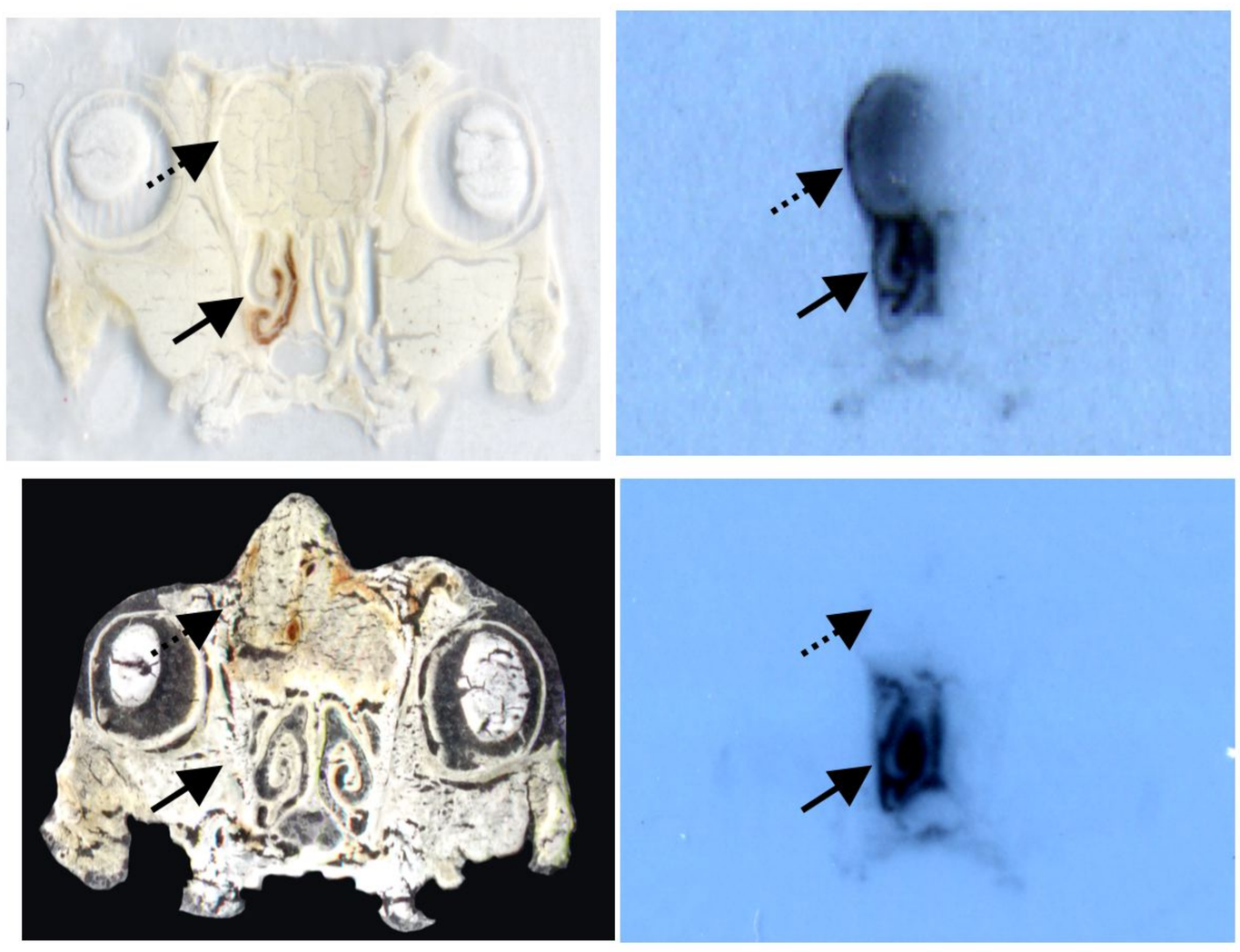

Control

BNTX Model

Mn-54

Control

BNTX Model

Figure 4

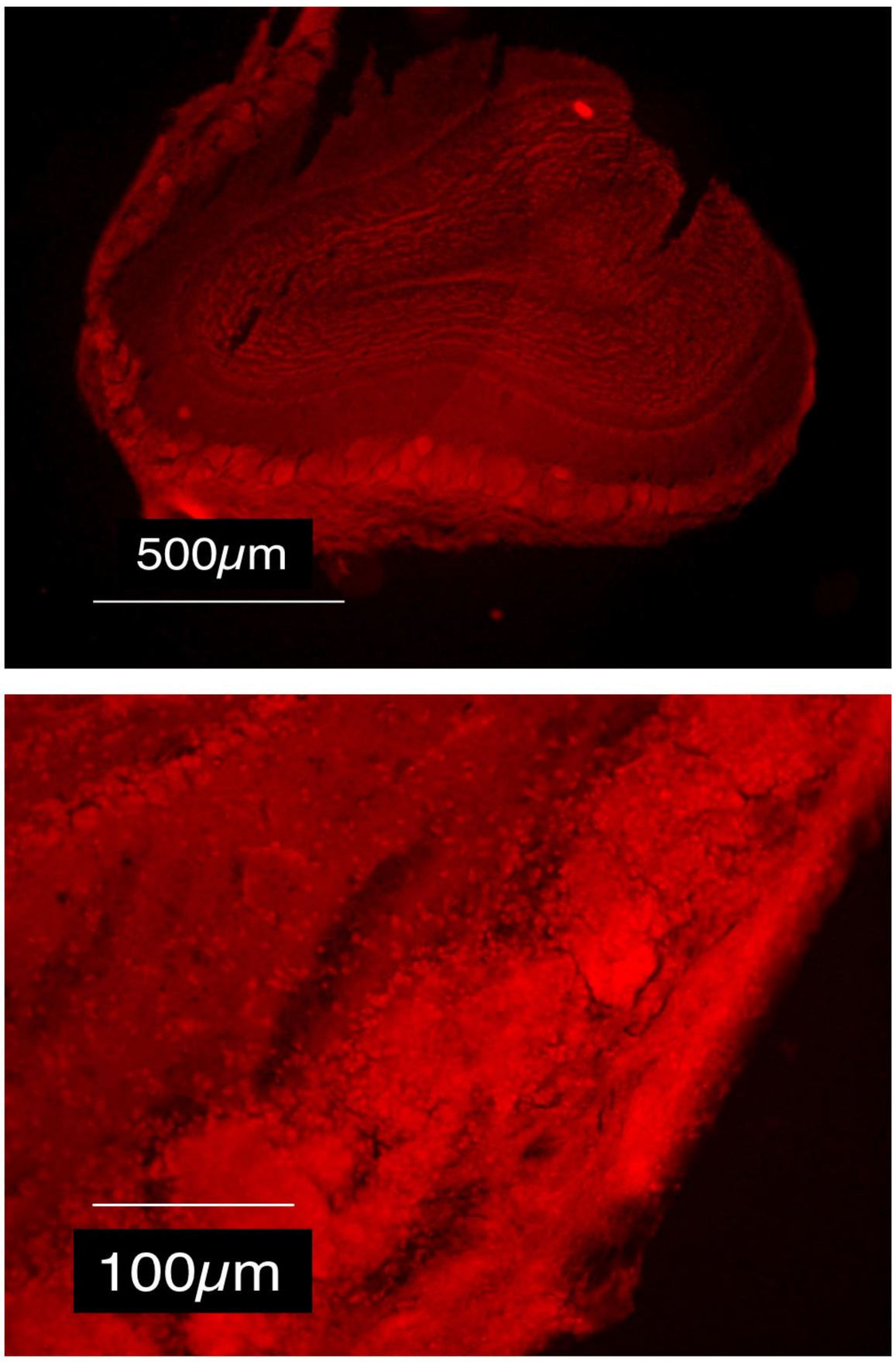

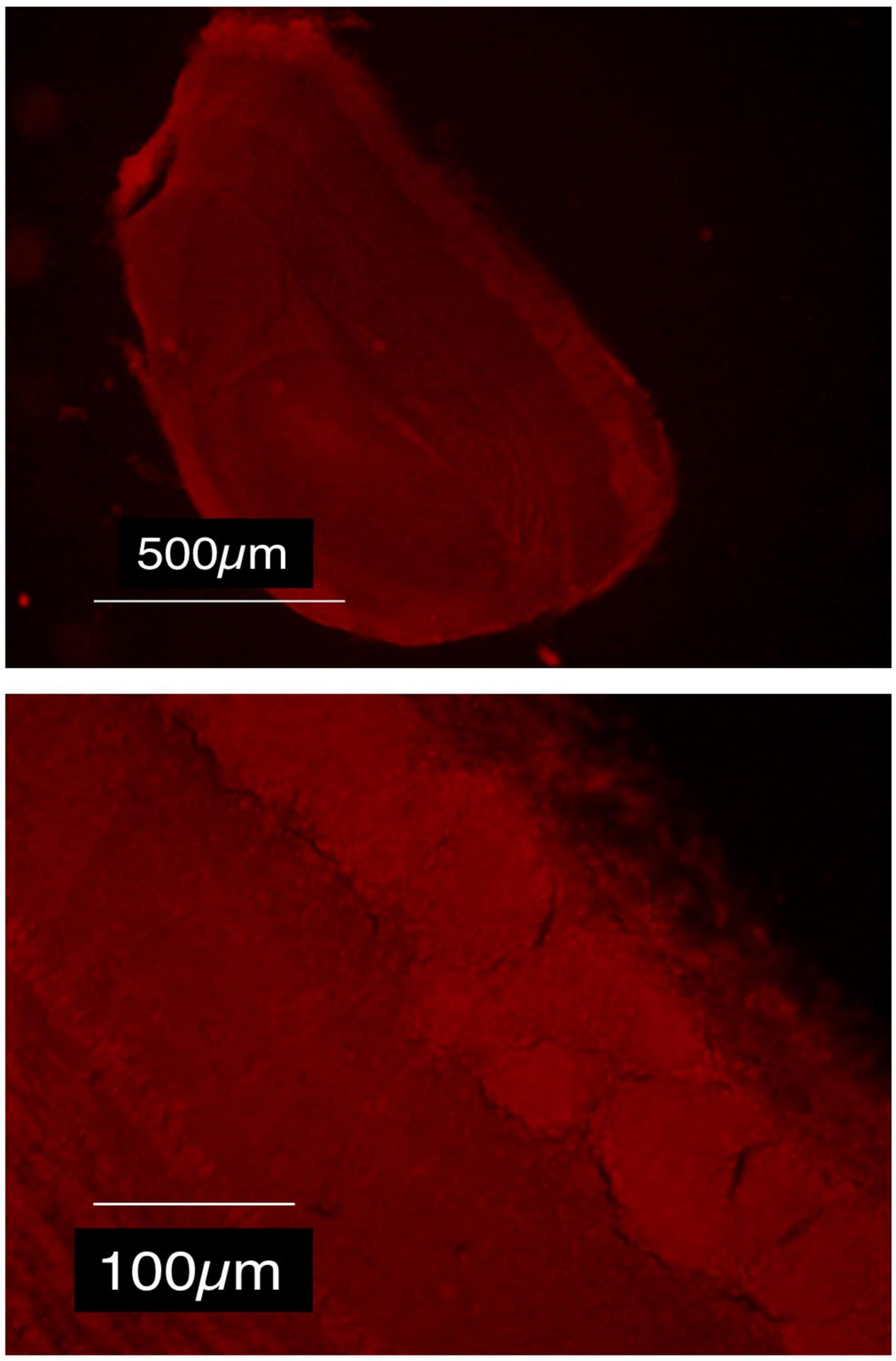

Control

BNTX Model